remote sensing

MDPI

Article

Changes in Vegetation Cover and the Relationship with Surface Temperature in the Cananéia–Iguape Coastal System, São Paulo, Brazil

Jakeline Baratto *, Paulo Miguel de Bodas Terassi and Emerson Galvani

Department of Geography, University of São Paulo, São Paulo 05508-000, Brazil; pmbterassi@usp.br (P.M.d.B.T.); egalvani@usp.br (E.G.)
* Correspondence: jakeline.baratto@usp.br

Abstract: The objective of this article is to investigate the possible correlations between vegetation indices and surface temperature in the Cananéia–Iguape Coastal System (CICS), in São Paulo (Brazil). Vegetation index data from MODIS orbital products were used to carry out this work. The Normalized Difference Vegetation Index (NDVI) and the Enhanced Vegetation Index (EVI) were acquired from the MODIS/Aqua sensor (MYD13Q1) and the leaf area index (LAI) from the MODIS/Terra (MOD15A2H). Surface temperature data were acquired from MODIS/Aqua (MYD11A2). The data were processed using Google Earth Engine and Google Colab. The data were collected, and spatial and temporal correlations were applied. Correlations were applied in the annual and seasonal period. The annual temporal correlation between vegetation indices and surface temperature was positive, but statistically significant for the LAI, with r = 0.43 (90% significance). In the seasonal period, positive correlations occurred in JFM for all indices (95% significance). Spatially, the results of this research indicate that the largest area showed a positive correlation between VI and LST. The hottest and rainiest periods (OND and JFM) had clearer and more significant correlations. In some regions, significant and clear correlations were observed, such as in some areas in the north, south and close to the city of Iguape. This highlights the complexity of the interactions between vegetation indices and climatic attributes, and highlights the importance of considering other environmental variables and processes when interpreting changes in vegetation. However, this research has significantly progressed the field, by establishing new correlations and demonstrating the importance of considering climate variability, for a more accurate understanding of the impacts on vegetation indices.

Keywords: vegetation indices; seasonal variation; MODIS/Aqua

check for updates

Citation: Baratto, J.; Terassi, P.M.d.B.; Galvani, E. Changes in Vegetation Cover and the Relationship with Surface Temperature in the Cananéia–Iguape Coastal System, São Paulo, Brazil. *Remote Sens.* **2024**, *16*, 3460. https://doi.org/10.3390/rs16183460

Academic Editors: Rui Yao and Mario Cunha

Received: 26 July 2024
Revised: 30 August 2024
Accepted: 13 September 2024
Published: 18 September 2024

1. Introduction

Vegetation is one of the main components of ecosystems and plays a key role in the analysis of global climate change and its impacts. Thus, the study of vegetation dynamics can provide important information about changes in vegetation cover and climatic attributes on a regional scale [1].

To understand vegetation dynamics over larger areas, remotely sensed vegetation indices are used as valuable tools to monitor vegetation [2]. Vegetation indices (VI) are widely used to identify the health of vegetation. In recent years, research using satellite-based VI, which seeks to characterize the response of vegetation to climate variability and changes in different areas, has become more recurrent [3].

The three most often used vegetation indices are the Normalized Difference Vegetation Index (NDVI), the Enhanced Vegetation Index (EVI) and the Leaf Area Index (LAI). These indices are widely accepted remote sensing metrics for monitoring vegetation growth and changes in cover [1], in addition to detecting vegetation health [4].

NDVI is sensitive to chlorophyll, while EVI responds better to canopy structural variations. The two vegetation indices are complementary in global and regional vegetation studies. EVI was developed to optimize the vegetation signal with greater sensitivity in regions of high biomass, providing better vegetation monitoring. This is achieved by decoupling the background signal from the canopy and reducing atmospheric influences [1,5,6].

The leaf area index (LAI) was defined as the integrated leaf area of the canopy per unit of projected soil surface (m^2/m^2) [7]. This index is calculated considering the surface area of just one of the leaf faces. Thus, LAI is a key biophysical parameter that determines the state of plant growth [8]. The LAI results from the ecophysiological responses of plants to the chemical, physical and biological conditions of the soil; microclimate conditions; and the interdependence of these factors in the different successional stages of vegetation [9,10].

In the climatic context, rainfall and surface temperature are the most used factors to understand vegetation dynamics. Periods of heavy rainfall can lead to greater plant growth and the expansion of vegetated areas [11]. For example, the study in the Hanjing River basin in central China, in which the authors demonstrated that rainfall was the dominant climate factor for NDVI change [12]. Research shows that NDVI has correlations with rainfall (P) and surface temperature (LST) [13]. Some studies, however, show that variation in vegetation indices (VI) may have insignificant correlations with climatic factors. For example, between rainfall and NDVI in the arid northwestern region of China [14]. Precipitation also did not show significant correlations with NDVI in the Upper Knoh River basin in the Himalayas. However, when using EVI, precipitation and other climatic and hydrological factors exhibited significant correlations. Thus, the authors suggest that EVI better captures changes in vegetation phenology than NDVI [15]. The study carried out in the tropical city of Raipur (India) also investigated the relationship between surface temperature and NDVI [13]. The authors' main conclusions were that the correlation between LST and NDVI was strongly negative (−0.51) on the vegetated surface, moderately positive in water bodies (0.45), and weakly positive in built-up areas and bare land (0.14).

NDVI was also the focus of study in the Gautam Buddh Nagar district, located in northern India [16]. The authors identified that the correlation between NDVI and LST (−0.45) was stronger than the other correlations analyzed, such as soil moisture ($r = 0.43$) and precipitation ($r = 0.341$). Thus, the results suggest that NDVI is more sensitive to LST compared to these other factors. The impacts of climate change and human activities on vegetation growth were investigated in the Hanjiang River Basin (China), during the 2001–2016 period [12]. The results produced by the authors indicated that areas with positive correlations between temperature and NDVI were relatively more dispersed throughout the study area. Additionally, only 1.8% of the area showed statistically significant negative correlations between temperature and NDVI.

EVI and NDVI were the focus of study in the Upper Knoh River basin in the Himalayas. The authors sought to evaluate the spatiotemporal variability of vegetation and associated climatic and hydrological factors in the river basin on annual and seasonal scales [12]; and the temporal variation of NDVI and LAI and their associations with hydroclimatic variables in the combined Sacramento and San Joaquin River basins in the United States [3]. The results produced by the authors suggest that NDVI and LAI have distinct relationships with hydroclimatic indicators. Furthermore, LAI is more strongly correlated with most of the hydroclimatic variables considered.

In Ethiopia, the spatial and temporal variability of NDVI and its response to potential evapotranspiration, rainfall, soil moisture and surface temperature in the Abbay River basin (Nile River tributary) was investigated [17]. The results demonstrate that NDVI was strongly correlated with the climatic variables, and that precipitation, temperature, potential evapotranspiration, and soil moisture have distinct effects on vegetation growth across various land use and land cover (LULC) categories and seasons. In the northeastern region, changes in vegetation cover as a function of surface temperature and rainfall were investigated from 2001 to 2020 [2]. In the northern region of Iran, the spatiotemporal relationship between MODIS EVI and climatic variables was also studied. The results show a significant spatial correlation between EVI and LST values, which was direct during winter and inverse during summer.

In Nigeria [18], the variation of vegetation and the correlation between precipitation and surface temperature were investigated in the humid and dry tropical regions. The results showed that NDVI had a negative correlation with temperature in 59.1% of the study area. The percentage of the region where NDVI had a positive correlation with temperature was 3.54%. NDVI was negatively correlated with temperature in six land cover types, including savannas, degraded forests, and Sahelian grasslands. However, the correlation analysis revealed a positive but weak association between temperature and NDVI in mangroves, forests, and forest vegetation.

In Brazil, studies on surface temperature are mostly limited to comparative studies with land use—such as in the Piracicaba region, São Paulo (Brazil)—focusing on grain production [19]; and in the Pontal do Paranapanema, located in western São Paulo (Brazil) [20]. Other studies seek to understand the relationship between anthropization and surface temperature warming, such as in the North Coast of São Paulo state (Brazil) [21]; and the spatiotemporal relationship between land surface temperature, green vegetation cover, and built-up areas in Brasília, Federal District, Brazil [22]. Additionally, some studies aim to evaluate vegetation and surface temperature during drought periods, such as in the Upper Paraíba River basin, a semi-arid region of Brazil.

Thus, satellite-based remote sensing products offer an interesting opportunity to analyze VI changes in response to climate change on a regional scale. Furthermore, this information can benefit regional ecological restoration and environmental conservation projects. In Brazil, especially in the southern coastal region of São Paulo, there is a research gap regarding the understanding of vegetation dynamics in response to surface temperature changes. Previous studies have focused on mangrove areas; for example, mangrove mapping [23,24] and mangrove microclimate [25–28]. Therefore, studies addressing climatic issues and vegetation variation are important in the region. In the study area, this becomes important due to the presence of environmental preservation with conservation units, in addition to the mangrove ecosystem, which serves as an important part of the ecosystem of society.

However, with climate change and shifts in air temperature and precipitation patterns, studies aiming to understand the relationship between surface temperature and vegetation could fill this gap and encourage further research to incorporate new methodologies, such as the use of remote sensing data, to understand vegetation patterns in the context of current climatic issues. Moreover, this study enhances the scientific community's understanding of the relationship between climatic variables and vegetation growth in ecosystems, particularly due to the importance of ecosystem services provided by preserved vegetation and mangroves in the study region. Therefore, the objective of this work is to investigate the possible correlations of vegetation indices (NDVI, EVI and LAI) with surface temperature in the Cananéia–Iguape Coastal System, SP.

2. Materials and Methods

2.1. Study Area

The Cananéia–Iguape Coastal System (CICS) is located on the southeastern coast of Brazil (Figure 1). The CICS is made up of three municipalities: Cananéia, Iguape and Ilha Comprida. Together, they have a current population of 54,823 inhabitants [29], with the majority residing in urban areas. The main economic activities in this region are banana farming and tea culture [30]. In addition, other important economic activities include aquaculture—which encompasses the breeding of fish, crustaceans and molluscs—and ecological tourism, which plays a significant role in generating local income [31].

The CICS's economic activities occupy an area of approximately 262 km^2, representing around 8% of the total area, as indicated by MapBiomas [32] mapping for the year 2022 (Figure 1C). Most of the region is covered by arboreal forest vegetation (35%) and arboreal restinga (45%). The predominant vegetation is dense ombrophylous forest, with submontane and montane subtypes, the latter being less predominant. The area occupied by mangroves corresponds to just 2% of the total. Other land uses include urbanized areas

(1%), flooded fields and swampy areas (2%), water bodies (5%) and herbaceous restinga (2%) [20].

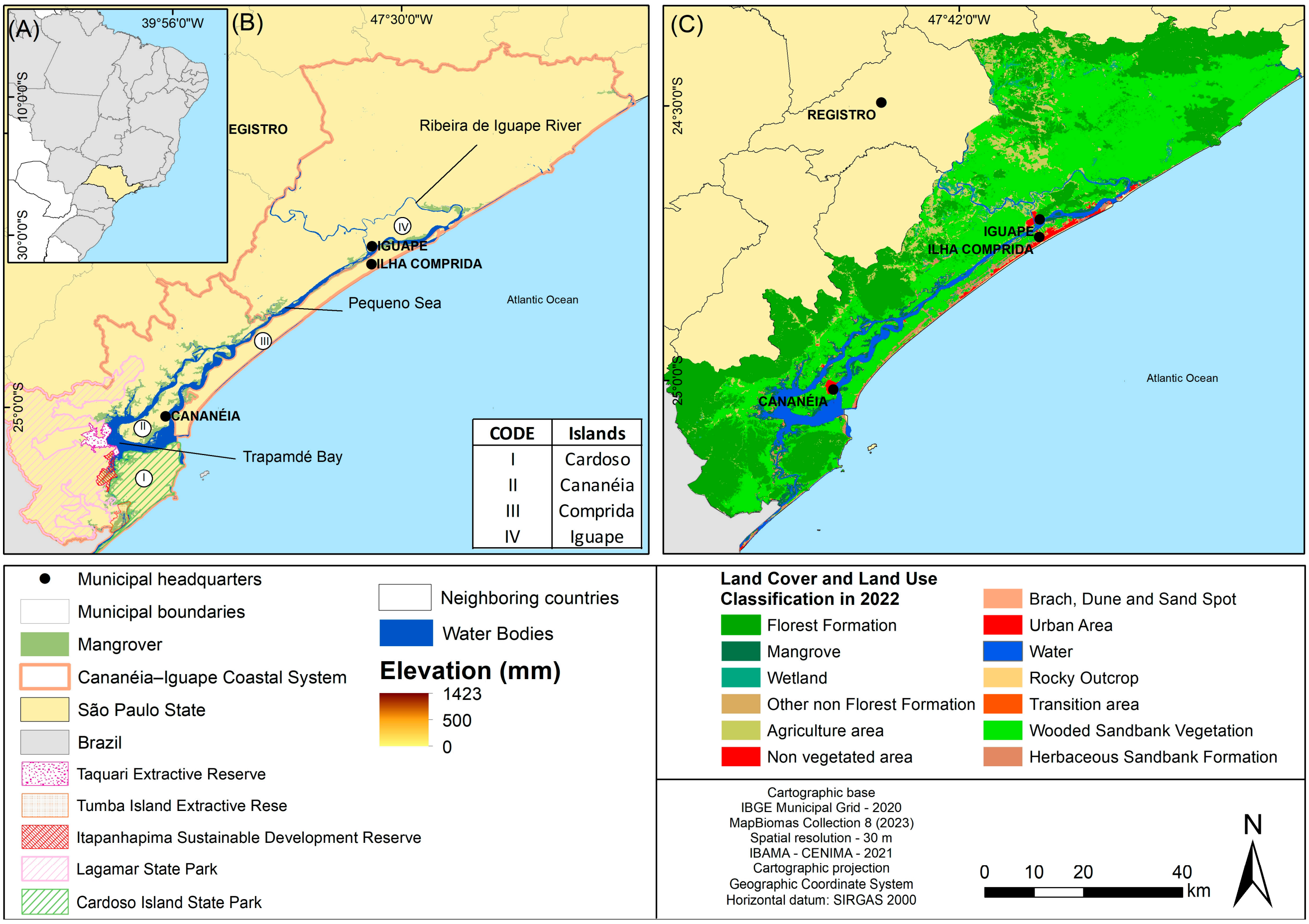

Figure 1. Location of the study area (**A**,**B**) and land use mapping (**C**).

The southern coast of the state of São Paulo is classified as the "Cfa" climate type, which defines a humid subtropical climate with a hot summer and no well-defined dry season, with the average temperature of the coldest month below 18.0 °C and the temperature of the hottest month above 22.0 °C [33,34].

The surface temperature (LST) corroborates the air temperature data, with the lowest temperature records occurring in the winter months (18.0 °C). In the summer months, the values are higher (25.0 °C)—(Figure 2A). Annually, the surface temperature did not show considerable fluctuations. Annual values were between 20.0 °C and 22.0 °C (Figure 2B).

Annual rainfall varies between 2000 mm and 3000 mm [35,36] along the CICS (Figure 2B). However, monthly rainfall presents lower values in the period from May to September [36]. In the historical series analyzed (2003–2022), it was observed that the month of August recorded the lowest rainfall (70.1 mm), while January had the highest volume (301.5 mm)—(Figure 2A). This lower volume during the winter period is attributed to the action of the Atlantic Tropical Anticyclone [37], while the highest volumes occur in summer due to air convection resulting from the greater incidence of sunlight and the action of intertropical atmospheric mechanisms (ZCAS) [38].

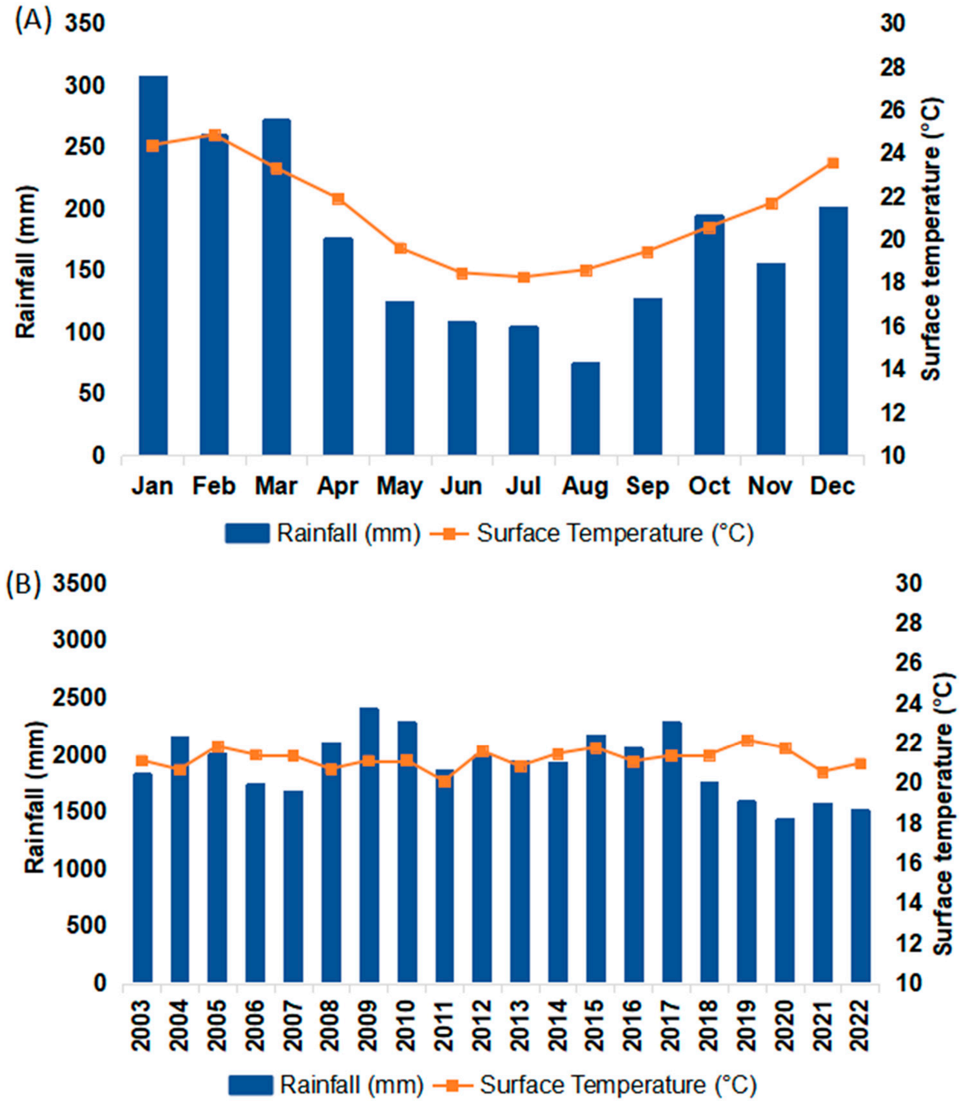

Figure 2. Variation in surface temperature and monthly (**A**) and annual (**B**) rainfall for the Cananéia-Iguape Coastal System for the 20032022 period. Source: MODIS/Aqua and CHIRPS, 2024.

2.2. Data Used

The data used in this research were obtained from the Moderate-Resolution Imaging Spectroradiometer (MODIS) sensor. The MODIS sensor has two receivers, Aqua and Terra, which orbit the planet every 1 or 2 days. The vegetation indices used were the normalized vegetation index (NDVI), enhanced vegetation index (EVI) and the Leaf Area Index (LAI). NDVI and EVI data was collected from the MODIS/Aqua receiver (MYD13Q1) [39]. This sensor collects images during the day and the night. The data are available at a temporal resolution of 16 days and a spatial resolution of 250 m [39], enabling broad and detailed coverage of the areas studied [40,41].

MODIS datasets are recognized for providing consistent, long-term information on vegetation characteristics [1], being widely used in environmental studies. Furthermore, these data are easily accessible and free, which makes it valuable for scientific research [1].

Leaf Area Index (LAI) data were obtained from the MODIS/Terra sensor (MOD15A2H). These data refer to an 8-day composite, with a spatial resolution of 500 m. The algorithm selects the "best" pixel available among all Terra sensor acquisitions over a period of 8 days [42].

Surface temperature (LST) data were acquired from the MODIS/Aqua satellite (MYD11A2) [43,44]. These data is available at 1:30 a.m. and at 1:30 p.m. (day/night) local time. It is provided with a spatial resolution of 1 km and a temporal resolution that corresponds to the average of 8 days of day and night data. This sensor has two temperature bands, daytime (LST_Day_1km) and nighttime (LST_Night_1km). To estimate the average daytime temperature, called LST, we used the average of these two bands, as reported in previous studies [5,45,46].

2.3. Data Processing and Analysis

The results were analyzed in two stages: temporal correlation and spatial correlation. The first step, the temporal correlation, was carried out in Python language on Google Colab, using the corr function (S1) for annual and seasonal data. The Pearson coefficient (r) was used as a correlation measure [5,10,47,48]. The annual correlation was calculated from the annual average data for the entire CICS region for the 2003–2022 period. Additionally, in the annual and seasonal temporal analysis, statistical analyses of the data were conducted, including calculations of the average, minimum and maximum values, standard deviation (σ), and coefficient of variation (CV) in Google Colab.

For seasonal correlation, the data were summed into seasonal averages for the LST, NDVI, EVI and LAI variables. These monthly averages were calculated for the periods: JFM (January, February and March), AMJ (April, May and June), JAS (July, August and September) and OND (October, November and December). To analyze the variability of the indices over time, the average value of all pixels in the CICS was calculated, as carried out in previous works [15].

In Google Earth Engine (GEE) [49,50], spatial correlation was performed between the values of the variables pixel by pixel. Surface temperature and LAI data were resampled to 250 m. To calculate the correlation, the ee.Reducer.pearsonsCorrelation reducer (S1) was used, which allows for obtaining Pearson's Linear Correlation (r) between the annual and seasonal values of the variables [10,48,51]. In this study, the correlation analysis was based on pixels, which means that each pixel has the correlation between vegetation indices and climate variables [15]. The spatial results were later manipulated in QGIS for more detailed analysis and the graphs were generated in Rstudio (2024).

3. Results

3.1. Temporal Correlation of Vegetation Indices with Climate Variables

3.1.1. Annual Temporal Correlation

The temporal analysis of vegetation indices revealed that annual values remained relatively stable in the CICS (Figure 3). The standard deviation for all indices analyzed was low, with an NDVI of 0.02, an EVI of 0.01 and an LAI of 0.20. Likewise, the coefficient of variation showed similar variation, with 2.1% for NDVI, 2.9% for EVI and 4.2% for LAI. The average NDVI and EVI values were 0.8 and 0.5, respectively. The maximum and minimum EVI values were 0.5 and 0.4, respectively, with 85% of years recording an EVI of 0.5 and 15% an EVI of 0.4.

The NDVI had a minimum value of 0.7 (5%) and a maximum value of 0.8 (95%). The year 2005 recorded the lowest NDVI and EVI values. The LAI showed similar variation, with a minimum value of 3.9 (2005), a maximum of 4.6 (2014) and an average value of 4.3, which represents 25.3% of the data. The correlations of annual values between NDVI and EVI values and LST were not statistically significant (p-value > 0.05) and were weak (Figure 4). Thus, LST showed a positive correlation with NDVI (r = 0.15) and EVI (r = 0.11).

Figure 3. Annual variation in vegetation indices for the 2003–2022 period in the Cananéia–Iguape Coastal System.

3.1.2. Seasonal Temporal Correlation

In seasonal periods (JFM, AMJ, JAS and OND), vegetation indices also showed little variation. The LAI showed a greater variation in the JFM and OND periods, with **σ** = 0.5 and CV = 10.2% and 13.6%, in that order, and lower in AMJ and JAS with **σ** = 0.4 and 0.3 and CV = 8.3%, in order. Considering the CV, the JAS and OND periods had higher values for NDVI and EVI, with CV between 4.3% and 5.3% (Table 1).

Table 1. Descriptive statistics for VI and seasonal periods in the Cananéia–Iguape Coastal System.

Period		**JFM**			**AMJ**			**JAS**			**OND**	
Variables	**NDVI**	**EVI**	**LAI**	**NDVI**	**EVI**	**LAI**	**NDVI**	**EVI**	**LAI**	**NDVI**	**EVI**	**LAI**
Average	0.8	0.5	4.6	0.8	0.5	4.6	0.8	0.4	4.0	0.7	0.5	4.0
Minimum	0.7	0.5	3.8	0.7	0.4	3.7	0.7	0.4	3.5	0.6	0.4	3.0
Maximum	0.8	0.5	5.6	0.8	0.5	5.2	0.8	0.5	4.6	0.8	0.5	4.7
Standard deviation	0.0	0.0	0.5	0.0	0.0	0.4	0.0	0.0	0.3	0.0	0.0	0.5
Coefficient of variation (%)	3.4	3.4	10.2	3.5	3.3	8.3	4.3	4.6	8.3	5.1	5.3	13.6

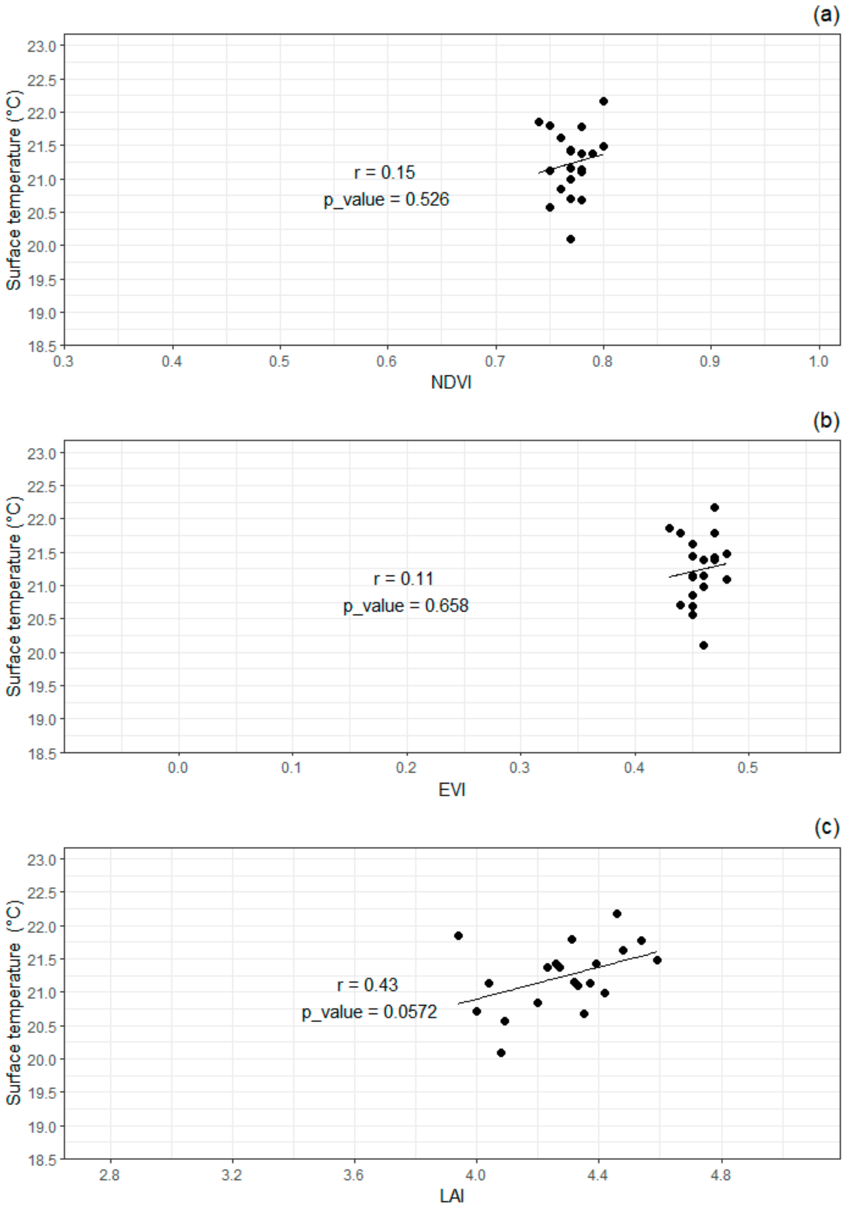

Figure 4. Scatter plot of annual NDVI (**a**), EVI (**b**) and LAI (**c**) values and surface temperature from 2003 to 2022.

The lowest NDVI value was 0.6 in the OND quarter (1.6% of the data). The highest NDVI value was 0.8 (76.3%). The EVI varied between 0.4 and 0.5, corresponding to 32.8% and 67.1%, in that order. Therefore, it is observed that the maximum values of EVI and NDVI corresponded to all months of the quarters.

The LAI showed greater variability in the CICS. The minimum value was 3.0 (1.3%) and the maximum value was 5.6 (1.3%). In the OND and JAS periods, the average LAI value was 4.0 and 5.2%, while in the JFM and AMJ periods, the average LAI value was 4.6 (9.2%).

In the AMJ (Figure 5) and JAS (Figure 6) quarters, the correlations between the NDVI, EVI and LST were weak and without statistical significance. However, the correlation of LAI and LST was 0.53 (p-value < 0.05) (Figure 6c). In the OND period, vegetation indices and LST had negative and weak correlations (EVI r = −0.15 and LAI r = −0.13) (Figure 6f). Also in this period, EVI has the best response compared to NDVI for CICS.

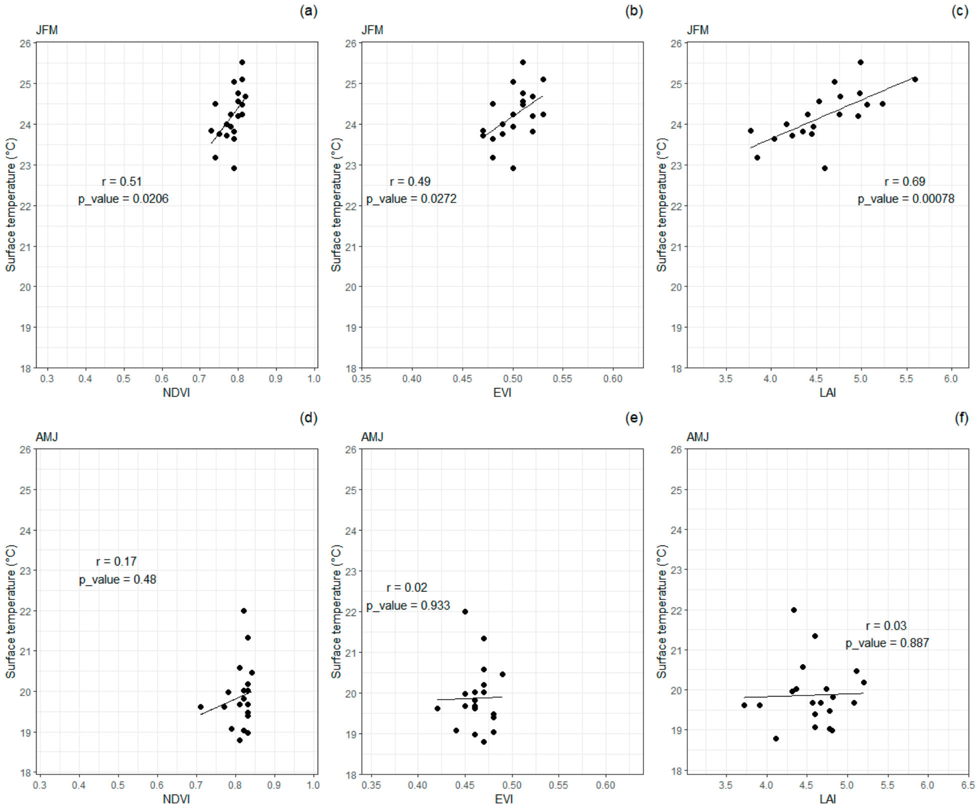

Figure 5. Scatter plot of seasonal values of VI–NDVI (**a**,**d**), EVI (**b**,**e**) and LAI (**c**,**f**)—and surface temperature for the JFM (**a**–**c**) and AMJ (**d**–**f**) quarter.

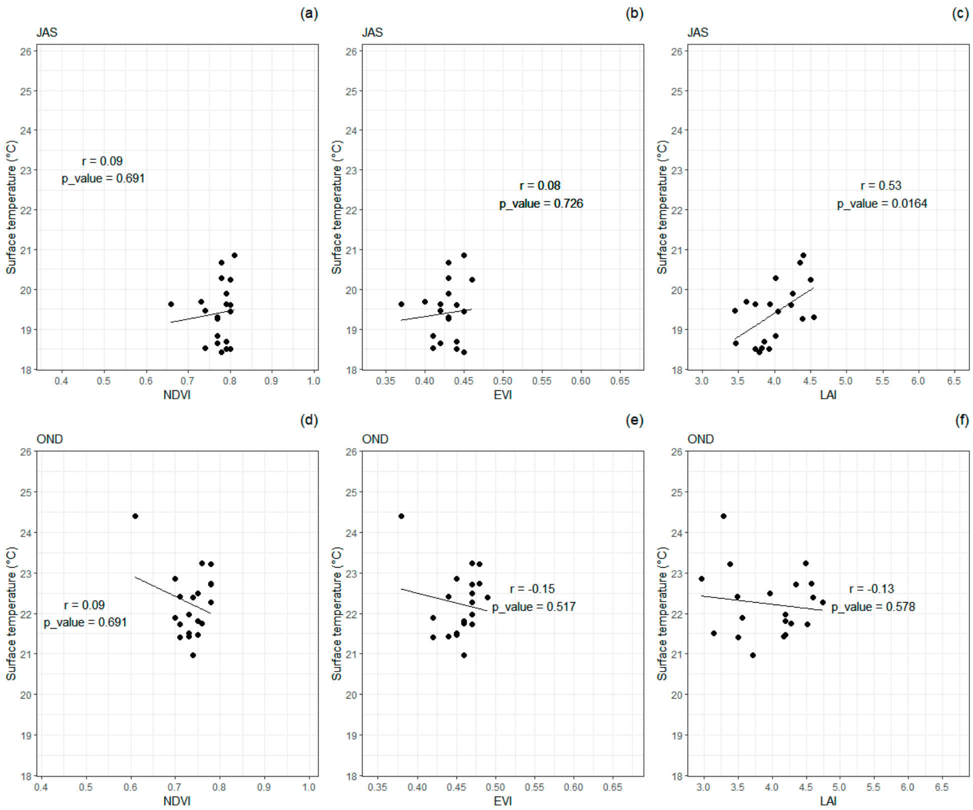

Figure 6. Scatter plot of seasonal values of VI–NDVI (**a**,**d**), EVI (**b**,**e**) and LAI (**c**,**f**)—and climate variables for the JAS (**a**–**c**) and OND (**d**–**f**) quarter.

3.2. Components Spatial Correlation of Vegetation Indices with Surface Temperature

3.2.1. Spatial Annual Correlation

Spatial correlation was applied to each pixel of the study area, at a spatial resolution of 250 m. Spatial correlation analysis revealed that small areas in the CICS showed significant correlations between vegetation indices and surface temperature (Supplementary Material 2). Positive and moderate correlations (0.40 to 0.69) between NDVI and LST occupied 6.6% of the area. These areas are in small portions of the CICS, mainly in the northern region (Figure 7). The negative correlations (1.4%) occurred close to the urban area of Iguape and in small areas in portions of land with agricultural cultivation, mainly, and with arboreal restinga (Figure 1B).

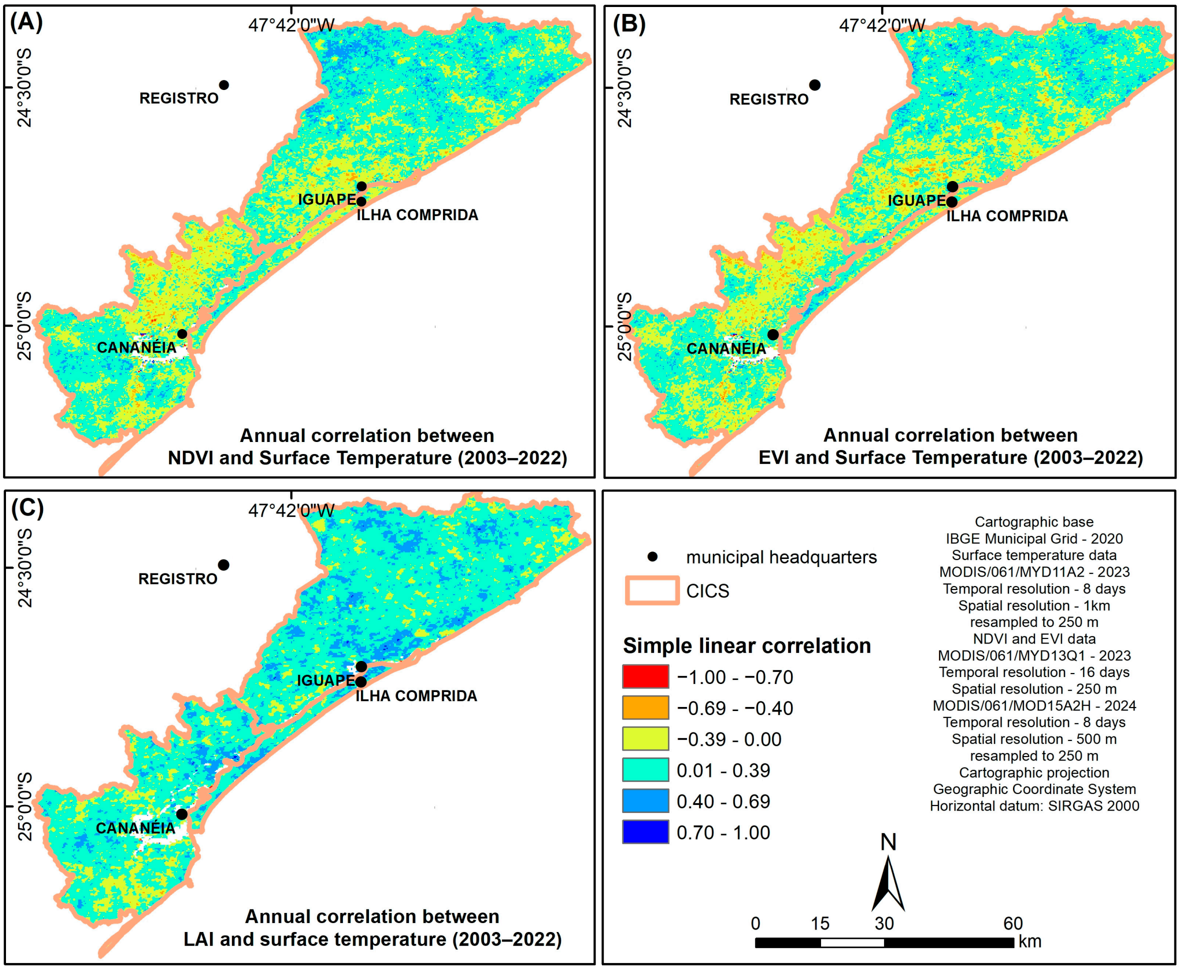

Figure 7. Annual linear correlation between surface temperature and NDVI (**A**), EVI (**B**) and LAI (**C**) between 2003 and 2022.

In relation to EVI, a positive and moderate correlation was observed in 4.5% (0.40 to 0.69) of the study area. The correlation is negative and moderate in 2.1% (0.69 to −0.40). The positive and moderate correlation was recorded in the northern sector of the municipality of Iguape, in an area with arboreal restinga and arboreal vegetation. Moderate (2.1%) and strong (0.1%) negative correlations are present near the Ribeira de Iguape river (Figure 1C) and in some areas where there is agricultural cultivation, such as pasture or plantation, in the municipality of Iguape (southern sector) and Cananéia (northern sector). Furthermore, some areas with negative and moderate correlation were observed in the south of the CICS.

The correlation of LST with LAI showed more expressive results. The correlation was moderate and positive in 14.5% of the area, mainly in the central sector of the CICS. The correlation was strong and positive at 0.1% of the CICS (Figure 7C). In the south of the CICS, areas with a negative correlation between LAI and LST were observed. This area is a region with a predominance of conservation units, being one of the most preserved areas in the CICS (Figure 1A).

3.2.2. Seasonal Spatial Correlation

In spatial seasonal correlations, it was observed that the largest area of the CICS does not present significant statistical correlations between VI and LST. However, some small areas had significant statistical relationships (Supplementary Material 2). Positive correlations between LST and LAI stand out in the JFM and JAS quarters, where the largest areas with significant correlations were identified. Thus, a positive and moderate correlation for LAI occurred in 53.3% of the area in JFM, and 22.3% in JAS.

In the JFM quarter (Figure 8A–C), the correlations between NDVI and LST were predominantly positive and moderate (14.8%). Positive correlations are in the extreme west and north of the CICS. These areas are dominated by arboreal forest and some areas with arboreal restinga, mainly in the municipality of Iguape. In the central region of the CICS, close to the city of Iguape, there is a negative correlation (0.9%). This contains areas of agricultural cultivation and arboreal restinga.

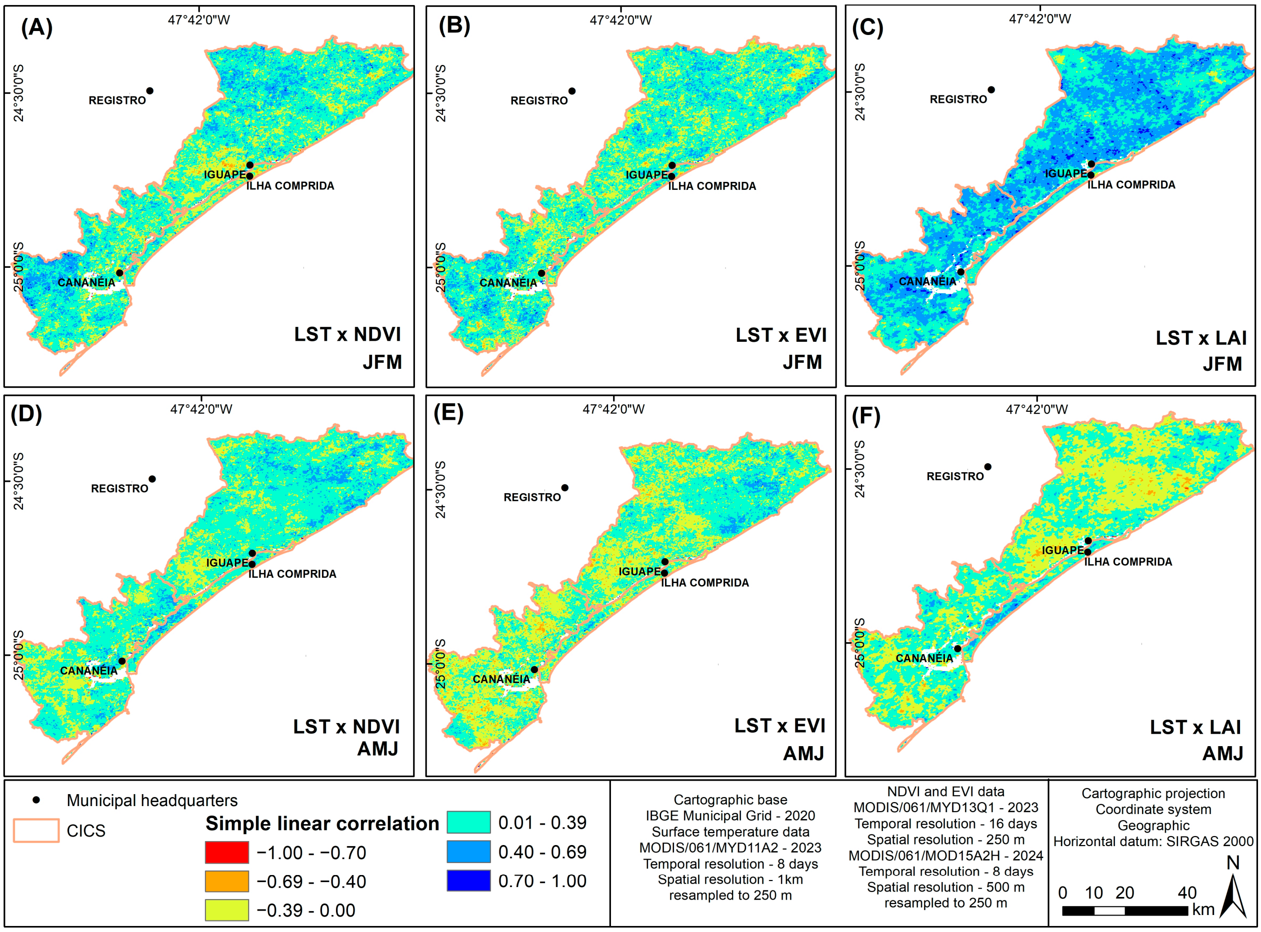

Figure 8. Seasonal linear correlation between surface temperature and VI between 2004 and 2022 for the JFM (**A**–**C**) and AMJ (**D**–**F**) periods.

The relationship between EVI and LST follows the same pattern as NDVI, with 11.7% of the area corresponding to a moderate positive correlation and 1.0% to a moderate negative correlation. The positive and strong correlation (0.2%) was observed in small areas in the central sector of the CICS, southwest and northeast, mainly in areas that generally occur in areas with arboreal forest vegetation. For the correlation between LST and EVI, negative correlations are found in the central sector, where the arboreal restinga and agriculture areas are located.

In the AMJ quarter, it was observed that negative correlations were more present in the study area for EVI and LAI. The areas with a negative correlation between EVI and LST (42.9%) were concentrated in the southern sector and in some areas of the northern region (municipality of Iguape), although without significance. In the south, this area corresponds to the transition from arboreal forest to arboreal restinga. In the north, the negative correlation is present around agriculture and arboreal restinga areas. Within these areas, the negative and moderate correlation values (2.4%) were significant. The NDVI also showed a reduction in significant correlation (Supplementary Material 2); however, in the northern sector and in the central region there were positive and moderate correlations (8.5%) and positive and strong correlations (0.2%). Positive correlations are present in the central sector, on the border between the three municipalities, where arboreal and herbaceous restinga occur.

Regarding the correlation of LAI and LST, the negative areas (1.2%) are in small partd of the northern sector. The areas with positive correlation (3.5%) are in the municipality of Cananéia, where herbaceous restinga and agriculture predominate (Figure 8F) in AMJ. Therefore, it was observed that there is a difference between correlations in seasonal periods.

In the JAS quarter, it was observed that the correlations between LST, NDVI and EVI had similar variations, with few areas with significant correlations (Supplementary Material 2). A negative correlation between NDVI and LST was identified in the southern sector of Cananéia and in the northern sector of Iguape (adding up to 1.0% of the area). A positive and moderate correlation (3.8%) occurred in the central sector of Cananéia and in the extreme west of Iguape (Figure 9A).

The correlation between LST and EVI presented the largest area with a positive and moderate correlation in the central sector of the CICS (2.6%). The positive correlation occurred in the same areas as the correlation between LST and NDVI, but in smaller proportions. For the LAI, the correlation between the LST and LAI identified that the northern sector has a positive and moderate correlation (22.3%), close to the correlation observed in JFM.

In the OND quarter, a positive and moderate correlation for LAI and LST occurred in 1.1% of the study area, differing from the other quarters analyzed. However, for this relationship, a negative and moderate correlation is found in the northeast and southwest sectors of the CICS, representing 4.2% of the area. However, the results found by LAI were closer to those found for the other indices in this quarter (Figure 9).

The correlation results identified that most of the CICS had weak negative correlations, being 53.1% (NDVI) and 51.6% (EVI). Negative and moderate correlations occurred in 9.8% and 7.4% of the CICS. These areas are mainly concentrated near the urban areas of Iguape and Cananéia. Furthermore, in the west of Iguape, a small area stands out with a strong negative correlation for NDVI and LST (Figure 9D). These correlations occur in places with the presence of arboreal restinga, arboreal vegetation and agriculture.

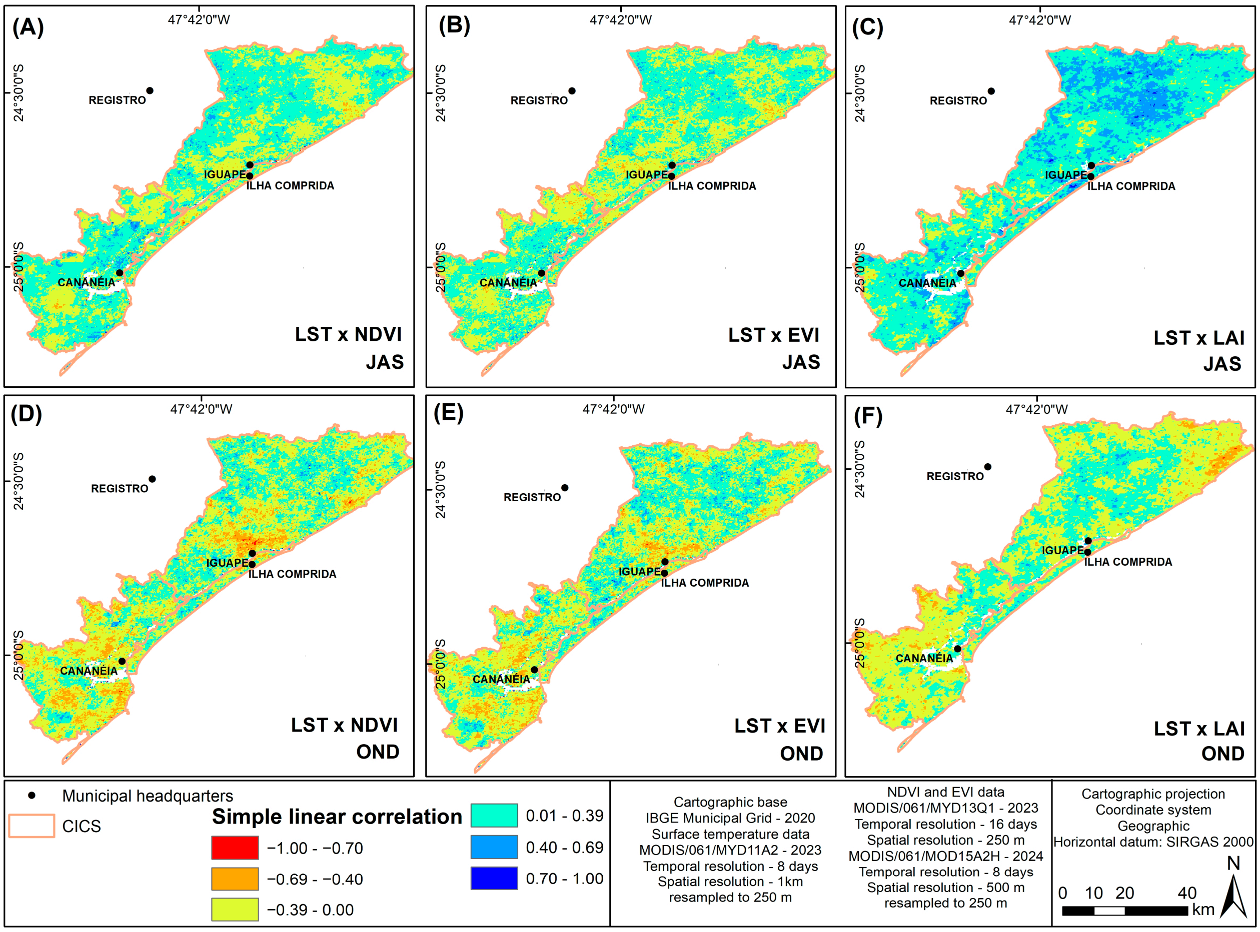

Figure 9. Seasonal linear correlation between surface temperature and VI between 2004 and 2022 for the JAS (**A**–**C**) and OND (**D**–**F**) periods.

4. Discussion

4.1. Temporal Correlation of Vegetation Indices with Climate Variables

Our results indicate that the IVs did not show significant variations in CICS. In other studies, the annual NDVI variation was higher; for example, in Brasília, where the minimum and maximum values ranged from −0.49 to 0.83, respectively. The highest NDVI values were observed for natural forests, particularly along streams [22]. In Nigeria, the average annual NDVI is 0.41 (ranging from 0.10 to 0.79) with a standard deviation of 0.12 for the entire country [18]. These differing results may be related to different land uses; in CICS, green areas with vegetation predominate, whereas in Brasília, there are more built-up areas. In Nigeria, the presence of different types of vegetation may have influenced this variation in NDVI.

Research in the Mongolia region (China) identified that the minimum EVI was 0.25 in 2021 and the maximum was 0.30 in 2012. Thus, the authors observed greater variability in EVI. Mongolia is in the transition zone from arid and semi-arid monsoon climates to humid and semi-humid climates [52]. This factor may be responsible for the lower EVI values, as were also found for the NDVI in Nigeria [18].

The EVI values found for the northern region of Iran were more similar to those of the CICS. The average EVI over 17 years (2000–2016) was about 0.45, with a maximum of 0.48 in 2011 and a minimum of 0.42 in 2000 [5]. The climate of northern Iran is considered very humid, humid, Mediterranean and western, central and eastern and mountainous semi-humid, respectively. Thus, the results in this region [5] are similar to the CICS results, due to the similarity of climatic characteristics, with the CICS also having a humid climate due to its proximity to the ocean.

For the Upper Khoh River Basin (UKR) in the Himalayas (India), we found the lowest EVI values. Average NDVI values range from 0.54 to 0.64, while the average EVI ranges from 0.31 to 0.35 [15]. The climate in the UKR is characterized by temperate conditions, with an annual rainfall of 1400 mm, concentrated between June and September, and average annual temperatures of 15.0 °C and 30.0 °C. The lower NDVI and EVI values for UKR are due to the difference in climate between the regions. Although average annual temperatures are approximate, the Upper Khoh River basin has temperatures close to zero in the highest regions during winter.

The difference between the NDVI and EVI values presented in these studies is because the EVI considers the effect of aerosol correction and canopy background adjustments that are not accounted for in the NDVI estimate [15,53,54]. These values disagree with those found in northern Iran, where the surface temperature, in annual data, indicated that the vegetation varies according to temperature fluctuations [5]. The results in Blkh province in northern Afghanistan showed that there is a strong and inverse correlation between NDVI and LST for annual mean values [48].

The relationship between NDVI and LST varies depending on land use [13]. The authors found that built-up areas and bare land present a positive and weak correlation with surface temperature. Furthermore, the relationship is moderately positive in water bodies. In the CICS, no significant correlations were found between the correlations, as the CICS has a large volume of water bodies, such as the Ribeira de Iguape River and Mar Pequeno (Figure 1B); this may have influenced the relationship between NDVI and LST. These values indicate that the vegetation is dense and does not present significant changes throughout the seasonal periods. Thus, no temporal seasonality was observed in the variation of NDVI and EVI for the CICS, disagreeing with the results of other research [15], where the greening of vegetation generally begins in May and reaches its maximum in September (NDVI) and August (EVI), and from this period it starts to decrease until April. Therefore, the higher LAI values in JFM and AMJ refer to the increase in rainfall that occurs in these periods, as shown in Figure 2A [35,36].

The results of the vegetation indices showed that the average vegetation in the CICS resulted in little variation during the analysis period. The high values indicate that the vegetation is dense and stable, showing little change over the years and quarters. However, changes in the NDVI variation are observed in different parts of the world, such as in northern Iran, where the trend is for an increase in EVI and NDVI [5]. Research on vegetation in the Khoh River basin also showed an increase in mean NDVI and EVI values [15]. Thus, the climatic factors of these regions can influence the variation of these indices. Furthermore, the type of vegetation also influences this variation. More arid regions, such as the northern Balk province of Afghanistan, have lower and more variable NDVI values, according to results found in another study [48]. Therefore, different climatic realities have an impact on the variation of VI, as observed in this research.

In the Gautam Buddh Nagar district (India), the average NDVI (2005–2018) in the study area was assessed at 0.45, indicating healthy vegetation. The highest and lowest monthly averages of NDVI were observed in February 2005 (winter month) and May 2010 (pre-monsoon month), respectively. The authors showed that the negative and significant correlation between NDVI and LST was for the pre-monsoon ($r = -0.61$), monsoon ($r = -0.65$) (rainy) and post-monsoon ($r = -0.87$) seasons [16]. The authors attribute this variation to the influence of climatic factors (precipitation and LST) on NDVI variation. Thus, the authors' results show that for India the NDVI responses are clearer compared to the CICS results.

Seasonal correlations between vegetation indices and LST were more significant. In the JFM quarter (Figure 5), the correlations between LST and vegetation indices were positive and statistically significant (p-value < 0.05). Although these results do not confirm most studies that indicate a negative correlation between NDVI and temperature [2] (Dastigerdi et al., 2024), the results indicate that a significant correlation occurred in the summer period. In this sense, some recent research has shown a positive correlation between NDVI and temperature [55]. The authors investigated the response of climate to NDVI variation in the Loess Plateau (China) and identified that NDVI was strongly positively correlated with temperature.

Positive results between LAI and LST were also found in another study [3]. The authors found a correlation of 0.46 between the LAI and temperature for the Sacramento and San Joaquin river basins (California, US). In addition to LAI, NDVI was positively correlated with LST. The authors attribute the positive correlation between average temperature and vegetation indicators to the fact that higher temperatures can make the environment more favorable for vegetation activity and, thus, promote higher NDVI and IAF, provided that adequate water is available.

Thus, the results indicated that temporal correlations between vegetation indices and climatic attributes were significant in the JFM and OND quarters. The months of AMJ and JAS did not obtain significant correlations. During these periods, higher volumes of precipitation occur (Figure 2). Thus, the positive correlation between vegetation indices and LST may be related to vegetation development, resulting in an increase in NDVI due to the availability of water and heat. Therefore, the positive correlation between NDVI and LST on the southern coast of São Paulo during the rainy summer is a result of the combination of high solar radiation, increased vegetation, intense evapotranspiration [18] and specific microclimatic characteristics of the region, such as proximity to the sea and low altitude. Even with the presence of rainfall, intense radiation and vegetative growth contribute to maintaining high LST, creating this positive correlation. Thus, land surface temperature is measured based on the physical interactions between energy and water flows in the surface–atmosphere system. Additionally, LST reflects local atmospheric conditions, surface type, soil moisture, and the vegetation's water balance [56].

In northern Iran, the spatiotemporal relationship between MODIS EVI and climate variables was studied, and it was identified that the correlation was significant between EVI and LST values, which was positive during winter (December to April) and inverse during the summer [5]. The results found in CICS indicate that the correlation is inverse in spring and positive in summer, disagreeing with other studies [5].

Some studies indicate a positive relationship between NDVI and LST, but in high-latitude regions [57] or in winter [58]. Correlations between LST and NDVI depend on the season and time of day [58]. The authors correlated NDVI with LST for North America. They identified that the correlation between NDVI and LST is positive in winter and negative in summer. Thus, other factors may be related to changes in NDVI [59] or also in different types of land use and cover [51].

For CICS, the correlation was positive in summer and in the remaining periods there were no significant correlations, although negative in OND, being more significant for EVI and LAI. Although the variables studied interfere with terrestrial photosynthetic activity and canopy structural variations [53], this relationship was not clear in the temporal correlation in the CICS for the annual periods and AMJ and JAS.

4.2. Components Spatial Correlation of Vegetation Indices with Surface Temperature

Thus, these results corroborate those identified for the Horn of Africa region [60]. The authors found that in areas with agricultural crops, the correlation was negative and significant between NDVI and temperature. In forest and wooded areas they were positively correlated. In Nigeria, areas with forest and mangrove vegetation also showed weak positive correlations. The authors conclude that moderate temperature ranges may enhance vegetation growth in humid regions. Our results partially corroborate these findings, indicating that in areas with vegetation, where NDVI is higher, LST is also higher. However, no pattern was observed in the spatial variation of the correlation between vegetation indices and LST in CICS. This suggests that other factors are influencing this correlation. Furthermore, land surface temperature is regulated by the amount of shortwave radiation absorbed by the surface, surface thermal conductivity, amount of water available for evaporative cooling, wind speed, and surface roughness, which regulate the strength of sensible and latent heat fluxes. Thus, these factors may influence the variation in LST in the study area [18].

These annual CICS results confirm those presented for the UKR river basin [15], that EVI has a strong correlation with different hydroclimatic factors compared to NDVI. Thus, the spatial correlation of the EVI was more significant for the CICS in some sectors, compared to the correlations between the NDVI. Therefore, EVI is an index more sensitive to changes in surface temperature, possibly because of aerosol correction and canopy background adjustments, which are not accounted for in the NDVI estimate [15]. However, the results found in this research differ from much of the work that seeks to understand the relationship between NDVI and LST [13,16,51,59–61].

These studies indicate that NDVI is negatively correlated with LST. In general, the results of this research indicate that most pixels, which comprise 61.2% of the area for NDVI, 65.2% of the area for EVI and 87.9% of the area for LAI, show a positive correlation between VI and LST. These results confirm the conclusions found in the Sacramento and San Joaquin River basins [3]. The authors identified that the positive correlation between LAI and LST provides a more favorable environment for vegetation activity.

The correlations between NDVI and EVI with LST were more similar and had correlations closer to the results highlighted in the literature [16] and those found in the temporal correlation for the quarter. Weak or non-existent correlations between NDVI and LST may be related to the presence of water in the study area. Therefore, the relationship between LST and NDVI is strongly effective in vegetation [13]. However, the relationship is positive (weak to moderate) in water bodies and weakly positive in the built-up area and exposed land. The authors found a negative correlation in all periods analyzed: pre-monsoon (r = −0.40, −0.51, −0.45), monsoon (r = −0.48, −0.41, −0.47), post-monsoon (r = −0.63) and winter (r = −0.12, −0.20, −0.18). In Nigeria, for example, areas with forest and mangrove vegetation also exhibited weak positive correlations, while negative correlations were found in savanna areas, settlements, degraded forests and Sahelian pastures. Thus, the type of vegetation and the presence of water can be crucial in the correlation between vegetation indices and LST. In CICS, the negative correlations, which confirm much of the research on the relationship between vegetation indices and LST, were mainly observed during the OND period. Thus, higher NDVI and EVI values are associated with lower LST values [18].

Furthermore, the relationship between NDVI and LST can change with changing land surface types [16,51,59,61]. The vegetation surface creates a strong correlation, and the force is reduced on the unvegetated land surface, the built-up surface and the water surface. The study for the city of Shanghai, China [51], identified that different types of land use and cover have significantly different effects on LST and NDVI. In the CICS, it was also observed that seasonal variation influences the spatial correlation between vegetation indices and LST. Thus, the hottest and rainiest periods have clearer correlations, such as in the OND and JFM periods. Considering this, it is observed that other factors, such as precipitation, may influence NDVI variation.

Thus, EVI tends to relate better compared to NDVI [15]. These authors also recommend using both vegetation indices to better understand the dynamics of seasonal and interannual vegetation, given the limitations of the different indices. The seasonal results found by this research disagree with the results found for the river basin UKR [15] and the annual results of the CICS. Thus, NDVI showed more visible correlations in seasonal periods compared to the annual scale results.

Seasonal spatial correlation indicated that areas close to water bodies and agriculture present negative relationships between LST, EVI and NDVI. Some areas covered by forest (dense ombrophylous forest) and arboreal restinga vegetation (Figure 1C) have a positive relationship. Therefore, some studies indicate that the relationship between LST and NDVI is influenced by the type of soil cover. Different types of land use and land cover have significantly different effects on LST and NDVI [51]. Furthermore, it is necessary to consider that rainfall also plays an important role in vegetation dynamics, which was not considered in this research.

5. Conclusions

This study showed that in the period analyzed (2003 to 2022), the vegetation indices (NDVI, EVI and LAI) had little temporal variation in the annual and seasonal period. The IVs (independent variables) show clearer responses in seasonal periods, particularly in summer, compared to the annual period. In summer, LST positively influences the variation in NDVI. Thus, the increase in LST is related to the increase in indices; however, this positive correlation may also be related to the presence of water and exposed soil. In turn, positive correlations in JFM months are also better adjusted to higher temperatures and greater total rainfall. However, further research is needed to support this statement.

In the spatial analysis, the LAI showed a clearer correlation in the JFM and OND periods, indicating that the increase in LST increases the LAI. Thus, temperature conditions can positively influence the photosynthetic activity of vegetation. The correlation between LST, NDVI and EVI indicate that the southern sector of the CICS and the central region have a negative correlation, and the northern sector has more areas with a positive correlation. This difference may occur due to different uses and land cover. Furthermore, the negative correlation in the cooler period (AMJ and JAS) indicates that the reduction in temperature decreases the photosynthetic activity of vegetation. In OND, there is an increase in temperature, and it is still a transition season to the rainy season.

However, in a large part of the CICS area, the correlations were not significant, which suggests that factors other than temperature may be influencing VI in the CICS region, such as rainfall and evapotranspiration. These factors also need to be investigated in future research to obtain more conclusive results. Thus, these results highlight the complexity of interactions between vegetation indices and climatic attributes and highlight the importance of considering a variety of environmental variables and processes when interpreting changes in vegetation.

Based on this, future research needs to consider climatic and hydrological variables such as precipitation, air temperature and evapotranspiration to find more accurate and precise results regarding vegetation variation in the CICS (Coastal Intertropical Convergence Zone). This research also did not consider vegetation types in the more detailed analysis of the correlation between the IVs (independent variables) and surface temperature. Thus, this gap could also be addressed in future studies.

Furthermore, it should be noted that understanding the correlation between climatic attributes and vegetation indices is little explored in this area of study. However, this research has significantly progressed this field, by establishing new correlations and demonstrating the importance of considering climate variability for a more accurate understanding of the impacts on vegetation indices. There is also the importance of satellite resources for advancing climatology research, as surface data are often scarce, which makes more in-depth studies on the topic unfeasible.

Supplementary Materials: The following is available online at https://www.mdpi.com/article/10.3390/rs16183460/s1, Supplementary Material 1: The scripts used to download the data and apply the correlations (https://doi.org/10.5281/zenodo.13768274), Supplementary Material 2: Figure S1. Maps of spatial variation of NDVI for the seasonal. Figure S2. Maps of spatial variation of EVI for the seasonal period. Figure S3. Maps of spatial variation of LAI for the seasonal period. Figure S4. Maps with *p*-values of annual and Figures S5 and S6. Seasonal correlations are available.

Author Contributions: Conceptualization, J.B.; methodology, J.B.; formal analysis, J.B.; investigation, J.B.; resources, J.B.; data curation, J.B.; writing—original draft preparation, J.B.; writing—review and editing, P.M.d.B.T.; visualization and supervision, E.G.; project administration, E.G.; funding acquisition, E.G. All authors have read and agreed to the published version of the manuscript.

Funding: The first author would like to thank FAPESP (Fundação de Amparo à Pesquisa do Estado de São Paulo) for granting the PDJ (process number n° 22/02383-3). The second author expresses gratitude to the Brazilian Coordination for the Improvement of Higher Education Personnel (CAPES) for granting the Doctorate Scholarship and to the Brazilian National Council for Scientific and Technological Development (CNPq) for the current Postdoctoral Grant (Process 165450/2020-7). The third author is grateful to the National Council for Scientific and Technological Development (CNPq) for the Research and Productivity grant (level 1D) process number 304973/2017-3.

Data Availability Statement: Data will be available upon request.

Acknowledgments: The first author thanks the following institutions: Fundação de Amparo à Pesquisa de São Paulo for funding this research. The third author thanks the National Council for Scientific and Technological Development (CNPq) for financial assistance through the Research and Productivity Research grant.

Conflicts of Interest: The authors declare no conflicts of interest.

References

1. Pradhan, B.; Yoon, S.; Lee, S. Examining the Dynamics of Vegetation in South Korea: An Integrated Analysis Using Remote Sensing and In Situ Data. *Remote Sens.* **2024**, *16*, 300. [CrossRef]
2. Dastigerdi, M.; Nadi, M.; Sarjaz, M.R.; Kiapasha, K. Trend Analysis of MODIS NDVI Time Series and Its Relationship to Temperature and Precipitation in Northeastern of Iran. *Environ. Monit. Assess.* **2024**, *196*, 346. [CrossRef]
3. Ukasha, M.; Ramirez, J.A.; Niemann, J.D. Temporal Variations of NDVI and LAI and Interactions with Hydroclimatic Variables in a Large and Agro-Ecologically Diverse Region. *J. Geophys. Res. Biogeosci* **2022**, *127*, e2021JG006395. [CrossRef]
4. Ponzoni, F.J.; Shimabuluro, Y.E.; Kuplich, T.M. *Sensoriamento Remoto da Vegetação*, 2nd ed.; Oficina de Texto: São Paulo, Brazil, 2012.
5. Sedighifar, Z.; Motlagh, M.G.; Halimi, M. Investigating Spatiotemporal Relationship between EVI of the MODIS and Climate Variables in Northern Iran. *Int. J. Environ. Sci. Technol.* **2020**, *17*, 733–744. [CrossRef]
6. Wang, J.; Fan, Y.; Yang, Y.; Zhang, L.; Zhang, Y.; Li, S.; Wei, Y. Spatial-Temporal Evolution Characteristics and Driving Force Analysis of NDVI in the Minjiang River Basin, China, from 2001 to 2020. *Water* **2022**, *14*, 2923. [CrossRef]
7. Watson, D.J. Comparative Physiological Studies in Growth of Field Crops. I Variation in Net Assimilation Rate and Learf Area between Species and Varieties, and within and between Yars. *Annatomy Bot.* **1974**, *38*, 41–76.
8. Zhao, J.; Wang, Y.; Zhang, H.; Zhang, Z.; Guo, X.; Yu, S.; Du, W. Spatially and Temporally Continuous LAI Datasets Based on the Mixed Pixel Decomposition Method. *Springerplus* **2016**, *5*, 516. [CrossRef]
9. Wandelli, E.V.; Marques Filho, A.O. Medidas de Radiação Solar e Índice de Área Foliar de Coberturas Vegetais. *Acta Amazon.* **1999**, *29*, 57–78. [CrossRef]
10. Wang, J.; Rich, P.M.; Price, K.P. Temporal Responses of NDVI to Precipitation and Temperature in the Central Great Plains, USA. *Int. J. Remote Sens.* **2003**, *24*, 2345–2364. [CrossRef]
11. Shi, L.; Fan, H.; Yang, L.; Jiang, Y.; Sun, Z.; Zhang, Y. NDVI-Based Spatial and Temporal Vegetation Trends and Their Response to Precipitation and Temperature Changes in the Mu Us Desert from 2000 to 2019. *Water Sci. Technol.* **2023**, *88*, 430–442. [CrossRef]
12. Yang, S.; Liu, J.; Wang, C.; Zhang, T.; Dong, X.; Liu, Y. Vegetation Dynamics Influenced by Climate Change and Human Activities in the Hanjiang River Basin, Central China. *Ecol. Indic.* **2022**, *145*, 109586. [CrossRef]
13. Guha, S.; Govil, H. Land Surface Temperature and Normalized Difference Vegetation Index Relationship: A Seasonal Study on a Tropical City. *SN Appl. Sci.* **2020**, *2*, 1661. [CrossRef]
14. Xuefei, L.; Guotao, D.; Huazhu, X. Spatial-Temporal Variation of NDVI and Its Responses to Precipitation in the Upper of Heihe from 2000 to 2019. In *Proceedings of the IOP Conference Series: Earth and Environmental Science*; IOP Publishing Ltd.: Zhangjiajie, China, 2021; Volume 783.
15. Kumari, N.; Srivastava, A.; Dumka, U.C. A Long-Term Spatiotemporal Analysis of Vegetation Greenness over the Himalayan Region Using Google Earth Engine. *Climate* **2021**, *9*, 109. [CrossRef]
16. Sharma, M.; Bangotra, P.; Gautam, A.S.; Gautam, S. Sensitivity of Normalized Difference Vegetation Index (NDVI) to Land Surface Temperature, Soil Moisture and Precipitation over District Gautam Buddh Nagar, UP, India. *Stoch. Environ. Res. Risk Assess.* **2022**, *36*, 1779–1789. [CrossRef]
17. Hussien, K.; Kebede, A.; Mekuriaw, A.; Beza, S.A.; Erena, S.H. Spatiotemporal Trends of NDVI and Its Response to Climate Variability in the Abbay River Basin, Ethiopia. *Heliyon* **2023**, *9*, e14113. [CrossRef]
18. Adepoju, K.; Adelabu, S.; Fashae, O. Vegetation Response to Recent Trends in Climate and Landuse Dynamics in a Typical Humid and Dry Tropical Region under Global Change. *Adv. Meteorol.* **2019**, *2019*, 4946127. [CrossRef]
19. Sayão, V.M.; dos Santos, N.V.; de Sousa Mendes, W.; Marques, K.P.P.; Safanelli, J.L.; Poppiel, R.R.; Demattê, J.A.M. Land Use/Land Cover Changes and Bare Soil Surface Temperature Monitoring in Southeast Brazil. *Geoderma Reg.* **2020**, *22*, e00313. [CrossRef]

20. Amaral Carrasco, R.; Maezano Faita Pinheiro, M.; Marcato Junior, J.; Ennes Cicerelli, R.; Antônio Silva, P.; Prado Osco, L.; Paula Marques Ramos, A. Land Use/Land Cover Change Dynamics and Their Effects on Land Surface Temperature in the Western Region of the State of São Paulo, Brazil. *Reg. Environ. Chang.* **2020**, *20*, 96. [CrossRef]
21. Wanderley, R.L.N.; Domingues, L.M.; Joly, C.A.; Da Rocha, H.R. Relationship between Land Surface Temperature and Fraction of Anthropized Area in the Atlantic Forest Region, Brazil. *PLoS ONE* **2019**, *14*, e0225443. [CrossRef]
22. De Oliveira, C.M.M.; Rezende, A.V.; Sano, E.E.; Matricardi, E.A.T.; Delgado, R.C. Spatiotemporal Assessment of Land Surface Temperature and Vegetation in Tropical Urban Areas. *Urban. Ecosyst.* **2023**, *26*, 45–65. [CrossRef]
23. Almeida de Oliveira, P.; Conti, L.A.; Nascimento Neto, F.C.; Barcellos, R.L.; Cunha-Lignon, M. Mangrove Individual Tree Detection Based on the Uncrewed Aerial Vehicle Multispectral Imagery. *Remote Sens. Appl.* **2024**, *33*, 101100. [CrossRef]
24. Conti, L.A.; de Araújo, C.A.S.; Cunha-Lignon, M. Spatial Database Modeling for Mangrove Forests Mapping; Example of Two Estuarine Systems in Brazil. *Model. Earth Syst. Environ.* **2016**, *2*, 73. [CrossRef]
25. De Lima, N.G.B.; Galvani, E. Interação Dos Atributos Climáticos Nos Manguezais Do Litoral Sul de São Paulo e Sua Relação Com Os Controles Climáticos. *Confins* **2018**, *36*, 1–21. [CrossRef]
26. De Lima, N.G.B.; Cunha-Lignon, M.; Galvani, E. Microclimatic Analysis of Mangroves in Two Distinct Categories of Protected Areas and Conserved Status. *Soc. Nat.* **2021**, *33*, e57483. [CrossRef]
27. Lima, N.; Cunha-Lignon, M.; Martins, A.; Armani, G.; Galvani, E. Impacts of Extreme Weather Event in Southeast Brazilian Mangrove Forest. *Atmosphere* **2023**, *14*, 1195. [CrossRef]
28. Galvani, E.; de Lima, N.G.B. Estudos Climáticos Nas Escalas Inferiores Do Clima: Manguezais Da Barra Do Rio Ribeira, Iguape, SP. *Mercator* **2010**, *9*, 25–38.
29. IBGE (Instituto Brasileiro de Geografia Estatística). Available online: https://cidades.ibge.gov.br/brasil/sp/cananeia/panorama (accessed on 29 August 2023).
30. Ross, J.L.S. A Morfogênese Da Bacia Do Ribeira Do Iguape e Os Sistemas Ambientais. *GEOUSP—Espaço Tempo* **2002**, *12*, 21–46. [CrossRef]
31. Dias, R.L.; de Oliveira, R.C. Caracterização Socioeconômica e Mapeamento Do Uso e Ocupação Da Terra Do Litoral Sul Do Estado de São Paulo. *Soc. Nat.* **2015**, *27*, 111–123. [CrossRef]
32. Souza, C.M.; Shimbo, J.Z.; Rosa, M.R.; Parente, L.L.; Alencar, A.A.; Rudorff, B.F.T.; Hasenack, H.; Matsumoto, M.; Ferreira, L.G.; Souza-Filho, P.W.M.; et al. Reconstructing Three Decades of Land Use and Land Cover Changes in Brazilian Biomes with Landsat Archive and Earth Engine. *Remote Sens.* **2020**, *12*, 2735. [CrossRef]
33. Alvares, C.A.; Stape, J.L.; Sentelhas, P.C.; De Moraes Gonçalves, J.L.; Sparovek, G. Köppen's Climate Classification Map for Brazil. *Meteorol. Z.* **2013**, *22*, 711–728. [CrossRef]
34. Beck, H.E.; Zimmermann, N.E.; McVicar, T.R.; Vergopolan, N.; Berg, A.; Wood, E.F. Present and Future Köppen-Geiger Climate Classification Maps at 1-Km Resolution. *Sci. Data* **2018**, *5*, 180214. [CrossRef] [PubMed]
35. Sant'Anna Neto, J.L. Ritmo Climático e a Gênese Das Chuvas Na Zona Costeira Do Estado de São Paulo-Brasil. *Rev. Bras. Geogr.* **1991**, *53*, 45–62.
36. Galvani, E.; Gilma, N.; De Lima, B.; Alves, R.R. Variabilidade e Tendência Das Precipitações No Litoral Sul de São Paulo. *Rev. Geonorte* **2012**, *1*, 1163–1176.
37. Reboita, M.S.; Alonso Gan, M.; Porfírio, R.; Rocha, D.A.; Ambrizzi, E.T. Precipitation Regimes in South America: A Bibliography Review. *Rev. Bras. Meteorol.* **2010**, *25*, 185–204. [CrossRef]
38. Reboita, M.S.; Ambrizzi, T.; Porfírio Da Rocha, R. Entendendo o Tempo e o Clima Na América Do Sul. *Terra Didat.* **2012**, *8*, 34–50. [CrossRef]
39. Didan, K. *MYD13Q1 MODIS/Aqua Vegetation Indices 16-Day L3 Global 250m SIN Grid V006*; NASA: Washington, DC, USA, 2013.
40. Phan, T.N.; Kappas, M.; Nguyen, K.T.; Tran, T.P.; Tran, Q.V.; Emam, A.R. Evaluation of MODIS Land Surface Temperature Products for Daily Air Surface Temperature Estimation in Northwest Vietnam. *Int. J. Remote Sens.* **2019**, *40*, 5544–5562. [CrossRef]
41. Tamiminia, H.; Salehi, B.; Mahdianpari, M.; Quackenbush, L.; Adeli, S.; Brisco, B. Google Earth Engine for Geo-Big Data Applications: A Meta-Analysis and Systematic Review. *ISPRS J. Photogramm. Remote Sens.* **2020**, *164*, 152–170. [CrossRef]
42. Myneni, R.; Knyazikhin, Y.; Park, T. *MODIS/Terra Leaf Area Index/FPAR 8-Day L4 Global 500m SIN Grid V061*; NASA: Washington, DC, USA, 2015.
43. Wan, Z. New Refinements and Validation of the Collection-6 MODIS Land-Surface Temperature/Emissivity Product. *Remote Sens. Environ.* **2014**, *140*, 36–45. [CrossRef]
44. Shiff, S.; Helman, D.; Lensky, I.M. Worldwide Continuous Gap-Filled MODIS Land Surface Temperature Dataset. *Sci. Data* **2021**, *8*, 74. [CrossRef]
45. Alqasemi, A.S.; Hereher, M.E.; Al-Quraishi, A.M.F.; Saibi, H.; Aldahan, A.; Abuelgasim, A. Retrieval of Monthly Maximum and Minimum Air Temperature Using MODIS Aqua Land Surface Temperature Data over the United Arab Emirates. *Geocarto Int.* **2022**, *37*, 2996–3013. [CrossRef]
46. Yu, P.; Zhao, T.; Shi, J.; Ran, Y.; Jia, L.; Ji, D.; Xue, H. Global Spatiotemporally Continuous MODIS Land Surface Temperature Dataset. *Sci. Data* **2022**, *9*, 143. [CrossRef] [PubMed]
47. Xu, J.; Fang, S.; Li, X.; Jiang, Z. Indication of the Two Linear Correlation Methods between Vegetation Index and Climatic Factors: An Example in the Three River-Headwater Region of China during 2000–2016. *Atmosphere* **2020**, *11*, 606. [CrossRef]

48. Qasimi, A.B.; Isazade, V.; Kaplan, G.; Nadry, Z. Spatiotemporal and Multi-Sensor Analysis of Surface Temperature, NDVI, and Precipitation Using Google Earth Engine Cloud Computing Platform. *Russ. J. Earth Sci.* **2023**, *22*, 1–12. [CrossRef]
49. Gorelick, N.; Hancher, M.; Dixon, M.; Ilyushchenko, S.; Thau, D.; Moore, R. Google Earth Engine: Planetary-Scale Geospatial Analysis for Everyone. *Remote Sens. Environ.* **2017**, *202*, 18–27. [CrossRef]
50. Mutanga, O.; Kumar, L. Google Earth Engine Applications. *Remote Sens.* **2019**, *11*, 591. [CrossRef]
51. Yue, W.; Xu, J.; Tan, W.; Xu, L. The Relationship between Land Surface Temperature and NDVI with Remote Sensing: Application to Shanghai Landsat 7 ETM+ Data. *Int. J. Remote Sens.* **2007**, *28*, 3205–3226. [CrossRef]
52. He, D.; Yi, G.; Zhang, T.; Miao, J.; Li, J.; Bie, X. Temporal and Spatial Characteristics of EVI and Its Response to Climatic Factors in Recent 16 Years Based on Grey Relational Analysis in Inner Mongolia Autonomous Region, China. *Remote Sens.* **2018**, *10*, 961. [CrossRef]
53. Huete, A.; Didan, K.; Miura, T.; Rodriguez, E.P.; Gao, X.; Ferreira, L.G. Overview of the Radiometric and Biophysical Performance of the MODIS Vegetation Indices. *Remote Sens. Environ.* **2002**, *83*, 195–213. [CrossRef]
54. Matsushita, B.; Yang, W.; Chen, J.; Onda, Y.; Qiu, G. Sensitivity of the Enhanced Vegetation Index (EVI) and Normalized Difference Vegetation Index (NDVI) to Topographic Effects: A Case Study in High-Density Cypress Forest. *Sensors* **2007**, *7*, 2636–2651. [CrossRef]
55. Li, P.; Wang, J.; Liu, M.; Xue, Z.; Bagherzadeh, A.; Liu, M. Spatio-Temporal Variation Characteristics of NDVI and Its Response to Climate on the Loess Plateau from 1985 to 2015. *Catena* **2021**, *203*, 105331. [CrossRef]
56. Coll, C.; Wan, Z.; Galve, J.M. Temperature-Based and Radiance-Based Validations of the V5 MODIS Land Surface Temperature Product. *J. Geophys. Res. Atmos.* **2009**, *114*, 1–15. [CrossRef]
57. Karnieli, A.; Agam, N.; Pinker, R.T.; Anderson, M.; Imhoff, M.L.; Gutman, G.G.; Panov, N.; Goldberg, A. Use of NDVI and Land Surface Temperature for Drought Assessment: Merits and Limitations. *J. Clim.* **2010**, *23*, 618–633. [CrossRef]
58. Sun, D.; Kafatos, M. Note on the NDVI-LST Relationship and the Use of Temperature-Related Drought Indices over North America. *Geophys. Res. Lett.* **2007**, *34*, 1–4. [CrossRef]
59. Han, W.; Chen, D.; Li, H.; Chang, Z.; Chen, J.; Ye, L.; Liu, S.; Wang, Z. Spatiotemporal Variation of NDVI in Anhui Province from 2001 to 2019 and Its Response to Climatic Factors. *Forests* **2022**, *13*, 1643. [CrossRef]
60. Ghebrezgabher, M.G.; Yang, T.; Yang, X.; Eyassu Sereke, T. Assessment of NDVI Variations in Responses to Climate Change in the Horn of Africa. *Egypt. J. Remote Sens. Space Sci.* **2020**, *23*, 249–261. [CrossRef]
61. Khan, Z.; Javed, A. Correlation Between Land Surface Temperature (LST) and Normalized Difference Vegetation Index (NDVI) in Wardha Valley Coalfield, Maharashtra, Central India. *Nova Geodesia* **2022**, *2*, 53. [CrossRef]